Journal of Nondestructive Evaluation manuscript No.
(will be inserted by the editor)

Local non-contact evaluation of the ac magnetic hysteresis parameters of electrical steels by the Barkhausen noise technique

Oleksandr Stupakov

Received: date / Accepted: date

Abstract The potential of the magnetic Barkhausen noise method for local repeatable testing of the magnetic hysteresis properties of electrical steels was investigated. Strips of non-oriented and grain-oriented electrical steels were magnetized by a single yoke through 0–10 mm air gaps. The measurements were performed at standard ac conditions: 50 Hz sine induction waveform with different amplitudes. A vertically mounted array of three Hall sensors was used for the *direct* measurement of the surface magnetic field. The Barkhausen noise was detected *locally* by a surface-mounted pancake coil. The simultaneous measurement of the actual sample field makes it possible to stabilize a recently introduced parameter, called Barkhausen noise coercivity. This parameter demonstrates strong linear correlations to the hysteresis coercive force and to the hysteresis losses measured by the standard single sheet tester.

Keywords Barkhausen noise · Magnetic hysteresis · Surface field measurement · Magnetization waveform control · Electrical steel

1 Introduction

Magnetically soft electrical steels are the basic material of the cores of transformers, generators and motors. Therefore, the ac magnetic properties of these steels are their main technological parameters of importance. Currently, the industry still requires a reliable magnetic testing system that can be applied on the production line for quality control. There is also a modern task to test

O. Stupakov
Institute of Physics, Academy of Sciences of the Czech Republic, v.v.i., Na Slovance 2, 18221 Prague, Czech Republic
Tel: +420-26605-2114
Fax: +420-28689-0527
E-mail: stupak@fzu.cz
URL: www.fzu.cz/˜stupak

the magnetic properties locally and at different magnetization angles relative to the rolling direction. In such on-line systems, the magnetization of the moving steel sheet and the detection of its magnetic response must be performed through a substantial and sometimes varied air gap between the magnet, the sensors and the sample. However, the accurate measurement of the magnetic hysteresis parameters in such a magnetically open configuration still presents a challenge (the well-known lift-off or contact problem) [1–3].

This work investigates the potential of the magnetic Barkhausen noise (BN) method for determining the ac magnetic hysteresis properties of the electrical steels [4,5]. The main advantage of the BN technique is that it can detect the magnetic response *locally* with a surface-mounted pancake coil [6,7]. The ultimate goal is to develop the BN system to the stage at which it can be applied for the industrial on-line control of steel quality.

This research was inspired by the preliminary results of dc measurements, which proved that the BN technique can be used for evaluation of the coercive force of the electrical steels. However, no correlation between the dc BN and the standard ac hysteresis parameters was found [3]. This work comprehensively investigated the case of ac BN measurements performed at standard industrial conditions. The same method of direct field measurement for accurate control of the *local* magnetization was used for stabilization of the BN response [3, 8,9]. An iterative digital feedback procedure was additionally developed to adjust the magnetization waveform to a standard sinusoidal shape [10]. Such controllable magnetization conditions were required for stable evaluation of the local surface coercivity by the BN method. Further principal result of this work is that this BN coercivity parameter demonstrated good linear correlations to the standard ac hysteresis data.

2 Experimental

Six different industrial grades of non-oriented (NO) electrical steels and six grades of grain-oriented (GO) electrical steels were used for the measurements [3]. The surface of the steel strips of standard sizes $300 \times 30 \times 0.25 - 0.5$ mm^3 were covered by an insulating coating of $\sim 5\ \mu m$ thickness. Two strips of each steel grade were magnetized by a large single yoke with the inner and the outer pole distances of 220 and 300 mm (see Fig. 1). An air gap between the yoke and the samples was varied in the range of 0–10 mm to determine the stability of the method. The measurements were then performed with the constant gaps of 3 and 5 mm for the NO and GO steels, respectively. The hysteresis measurements were also conducted for the standard configuration of the single sheet tester (SST): the strips inside a homogeneously wound magnetization coil were pressed at their ends by two attached yokes of the same size [11].

The technical details of the setup have been comprehensively discussed in a previous study [10]; only the necessary experimental parameters are specified below. The magnetic induction B was evaluated by a numerical integration

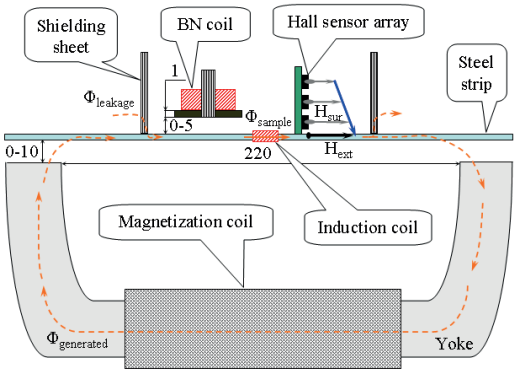

Fig. 1 Scheme of measurement setup (shown sizes are in mm).

of the signal induced in a sample-wrapping coil. According to the standard requirements, the $B(t)$ waveform was iteratively adjusted to the sine curve by means of a digital feedback procedure [5]. The measurements without the $B(t)$ waveform control (with the sinusoidal magnetization voltage) were also performed for comparison. The results of the measurements with and without the $B(t)$ control were found to be qualitatively similar. So by default, the results in the next section are presented for the more accurate measurements with the controlled $B(t)$ waveform.

The NO steels were measured at fixed induction amplitudes $B_{max} = 1$ and 1.25 T; the GO steels were measured with $B_{max} = 1.25$ and 1.5 T (the industrially attractive levels of low and middle saturations). The magnetization frequency f was settled to the power line frequency of 50 Hz. The experiments were repeated for the opposite sample side to verify the stability of the direct field measurement. Two typical NO and two typical GO steel strips were additionally tested in the wide ranges of induction amplitudes and magnetization frequencies: $B_{max} = 0.1 - 1.5$ and $0.1 - 1.8$ T for the NO and GO steels, respectively, at three different magnetization frequencies $f = 25, 50$ and 100 Hz; $f = 1 - 100$ Hz at fixed $B_{max} = 1, 1.25$ and 1.5 T for the NO and GO steels, respectively.

A tangential surface field profile at 1.5, 4.5 and 7.5 mm above the sample was measured by a vertically mounted array of three Hall sensors. Modern Hall chips with a 5 mV/G sensitivity and a sensitive area of approximately 0.1×0.1 mm^2 were used. Noisy output signals from the Hall sensor were smoothed by averaging the subsequent magnetization cycles: 3000 and 5000 cycles for the NO and GO steels, respectively. A "shielding" approach was used for the suppression of the field gradient: two GO steel sheets forced the magnetic leakage flux to flow through the sample [10]. The actual sample field was determined by linear extrapolation of the measured field profile to the sample face (see Fig. 1) [8]. All the magnetic parameters were evaluated for three different methods of field determination: the extrapolated field H_{ext}, the

surface field H_{sur} measured by the closest Hall sensor at 1.5 mm distance above the sample and the standard current field $H_i = NI/l_m$ (N is the number of turns of the magnetizing windings, I is the magnetization current read from a shunt resistor and $l_m = 220$ mm is the inner distance between the yoke poles by analogy with the SST standard) [3,9,11].

The BN was measured separately by a surface-mounted pancake coil of 1000 turns with a core made from laminated GO steel and encased inside a Cu-shielded grounded case [7]. The cross-section of the core was 4×4 mm^2, and the outer diameter of the coil was 16 mm. The BN coil was positioned near the Hall sensor array as shown in Fig. 1. The BN signal was amplified by 2–5 thousand times, band-pass analog filtered, digitized at a 500 kHz sampling rate and digitally filtered in the bandwidth of 2-50 kHz (the resonance frequency of the coil was about 120 kHz). Then the rms profile of the sampled signal (BN envelope) was calculated, averaged over $\sim$ 10 adjacent points to 1000 experimental points per one magnetization cycle and finally averaged over 500 subsequent magnetization cycles. The BN signal was sampled together with the magnetization current to determine the correlation with the previously measured hysteresis data [8]. The lift-off height of the BN coil was varied over the range of 0–5 mm to investigate the stability of the BN parameters. The measurements were then performed with a constant "zero" gap, which includes the strip insulating coating and a 1 mm thickness of the BN coil bobbin (see Fig. 1). A set of various BN parameters (BN rms value, BN envelope, BN energy, number of BN counts, etc.) was evaluated for a detailed analysis [7].

3 Results

Fig. 2(a) presents the BN envelopes measured with the different BN coil lift-offs. The observed two-peak behavior is typical for the magnetically soft materials [3,5]. A dynamic phase shift between the output BN signal and the applied magnetic field leads to a kink of the envelope at positive saturation. Fig. 2(a) clearly illustrates that despite a rapid decrease of the BN signal with the lift-off height, the shape of the BN envelope remains nearly constant. Small deviations in the saturation regions are probably caused by higher influence of a parasitic background noise on the weaker BN signal measured with the 3 mm lift-off.

Therefore, the BN parameters describing the signal shape should be generally more stable than the parameters describing the absolute level of the BN signal. Such a shape-based parameter was introduced recently by analogy with the traditional hysteresis coercive force, H_c, which is defined as the applied field intensity required to reduce the material magnetization to zero after the sample magnetization [9,11]. In this way, the intersection of the time integral of the BN envelope (a BN loop) with the field axis was called a BN coercivity, BN H_c [3,8,12]. To obtain the hysteresis-like loop from the positive rms envelope, the descending magnetization branch was reversed to the negative region (see Fig. 2(b)).

(a) (b)

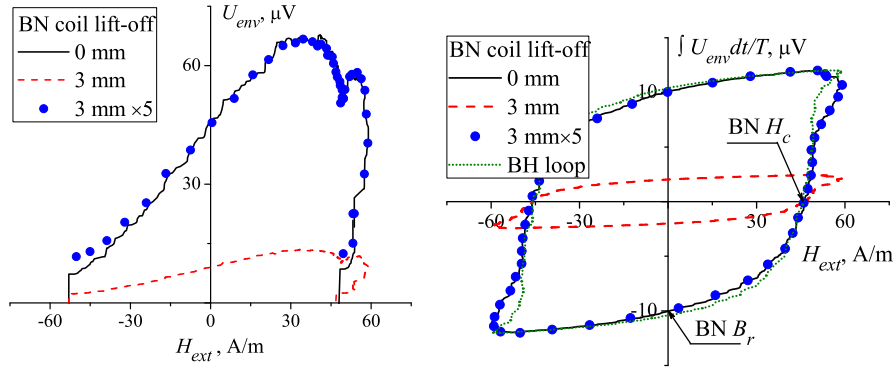

Fig. 2 (a) The BN envelopes, U_{env}, of the typical NO steel as a function of the extrapolated field, H_{ext}. The measurements were performed for 0 and 3 mm lift-off heights of the BN coil; $B_{max} = 1$ T. The circular symbols present the data for the 3 mm lift-off scaled up to 5 times. (b) The corresponding BN loops (time integrals of the BN envelope normalized to the magnetization period T) as a function of H_{ext}. The introduced BN coercivity, BN H_c, and the BN remanence, BN B_r, are shown by the arrows. The hysteresis BH loop with a normalized induction axis is also shown for comparison.

Fig. 3(a) confirms the stability of the BN H_c with respect to the BN coil lift-off height. Whereas the BN rms value decreases by more than 80%, the measurement error of the BN H_c is within 1% for all three of the methods of magnetic field determination. However, the physically accurate method of surface field extrapolation demonstrates the highest stability and an extraordinary level of experimental error within 0.2%.

The control of the induction waveform $B(t)$ with the simultaneous direct determination of the field dependence $H_{sur}(t)$ and $H_{ext}(t)$ additionally stabilizes the measurements with different air gaps between the yoke and the samples (see Fig. 3(b)). The H_{sur} values are a slightly smaller than the H_{ext} values due to a small negative gradient of the surface sample field [11]. However, the current field H_i data are not stable because of an increasing demagnetizing field [3,10]. The measurements without the $B(t)$ waveform control show similar stability with the air gap, but considerably higher values of BN H_c than that obtained with the sinusoidally controlled $B(t)$ waveform. The absolute values of the BN H_c are slightly higher than that of the hysteresis coercive force (see also Fig. 2(b)).

The dependence of the BN H_c on the hysteresis coercive force, H_c, for the NO steels and all three of the methods of field determination are shown in Fig. 4(a). No pronounced dependence was found for the current field H_i data measured with the yoke-sample gap of 3 mm. However, the direct field data, H_{ext} and H_{sur}, demonstrated perfect linear correlations with small offsets of approximately 1-2 A/m and almost unit slopes. This finding was definitely confirmed by the additional measurements with different induction amplitudes,

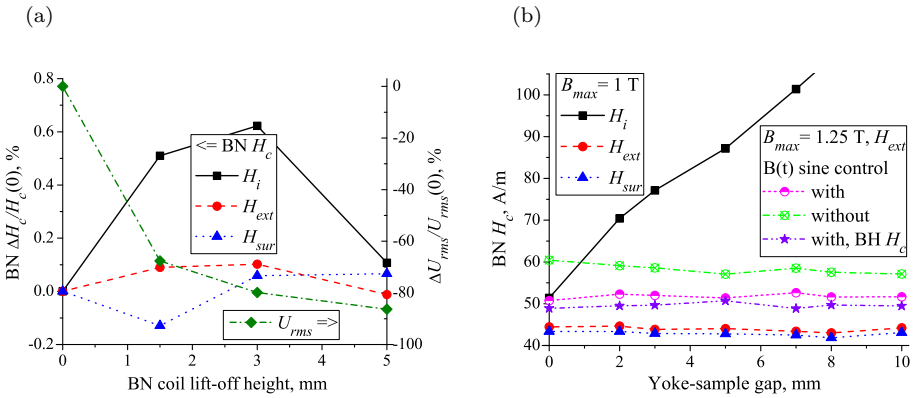

Fig. 3 (a) Normalized relative changes of the BN coercivity, BN H_c, (left scale) and the BN rms value, U_{rms}, (right scale) with the BN coil lift-off height. The data were normalized to the values obtained with the zero lift-off height. The BN H_c curves are shown for the three methods of field determination. (b) Variations of the BN H_c with the gap between the yoke and the sample. The relationships are shown for the different induction amplitudes, B_{max}, and the field representations, with and without the $B(t)$ waveform control. The curve for the hysteresis coercive force, BH H_c, in the H_{ext} representation is also shown for comparison. The measurements were performed on the typical NO steel.

B_{max}, and magnetization frequencies, f. The coercivity correlations were also proved to be independent of the magnetization frequency f (see Fig. 4(b)) [3, 12].

The relationship with the SST data is similar to that for the direct field measurements; however, the accuracy of their linear fits is slightly worse (compare Figs. 4(a) and 5(a)). Similar linear correlations of the BN H_c to the hysteresis losses W were obtained. However, these linear correlations are already dependent on the induction amplitude value B_{max} (see Fig. 5(b)). The linear correlations for the softer GO steels appear to follow the linear correlations of the NO steel data, but with higher scattering in much lower range of magnetic parameter variation for the different steel grades. E.g., H_c for the NO steels differs in the range of 50 A/m, whereas, for the GO steels, it varies in the narrow range of 7 A/m (see Fig. 5(a)). The additional measurements with different B_{max} and f values verified the reliability of our experimental data. With wider range of parameter variation, good linear correlations to the corresponding SST quantities were obtained for the GO steel as well. The dependence of the coercivity-loss correlations on the B_{max} value was also proved; the relation obtained with the fixed f and varied B_{max} illustrated this fact clearly (see Fig. 6) [11].

Similar to the BN coercivity, a BN remanence (a value of the BN loop at zero magnetic field), BN B_r, and BN losses (an area of the BN loop), BN W, can also be introduced (see Fig. 2(b)) [3]. These parameters demonstrate poor correlations to the corresponding hysteresis quantities for the different tested steels as compared to the BN H_c. For the GO steels, there are no correlations for the BN remanence (see Fig. 7). However, there is a noticeable trend for

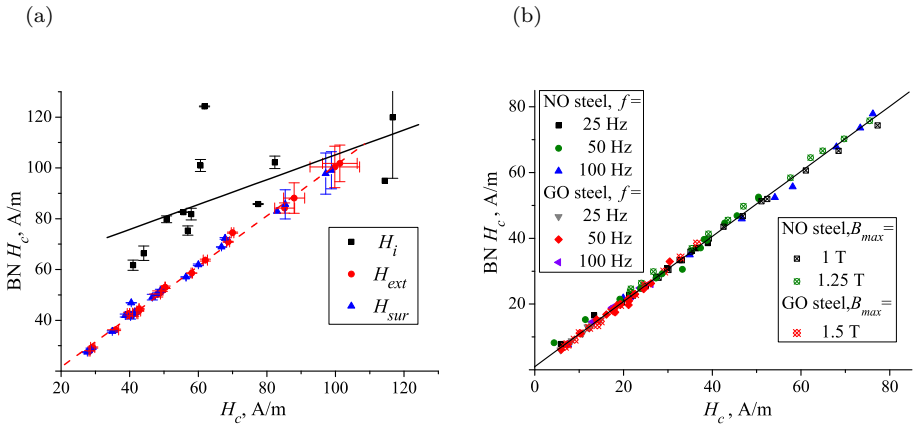

Fig. 4 Dependence of the BN coercivity, BN H_c, on the hysteresis coercive force, H_c, measured in the single yoke configuration. In figure (a) the data for the NO steels, both induction amplitudes and the three field methods are shown. The error bars represent the standard error of two identical tests from the opposite sample sides. The best linear fit for the H_{ext} data is $y = 1.73 + 0.993x$ (dotted line); the corresponding Pearson correlation coefficient $R = 0.998$ and the standard deviation $SD = 1.34$. In figure (b) the extrapolation field data are presented for the typical NO and GO steels measured at different B_{max} and f values. The fixed values of B_{max} and f are shown in the graph labels. The best linear fit is $y = 0.97 + 0.9899x$; $R = 0.9981$ and $SD = 1.097$.

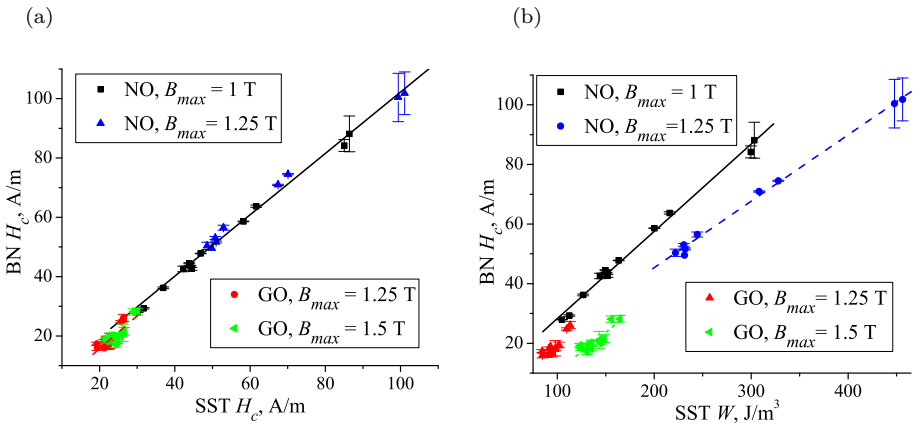

Fig. 5 Dependence of the BN H_c on the SST coercive force, H_c, (a) and on the SST hysteresis losses, W (b). The extrapolation field data are shown for all the steels, both B_{max} values and the fixed $f = 50$ Hz. In figure (a) the linear fit for the NO steels is $y = -1.24 + 1.035x$, $R = 0.9968$ and $SD = 1.74$ (solid line); for the GO steels, it is $y = -6.35 + 1.104x$, $R = 0.849$ and $SD = 1.92$ (dotted line).

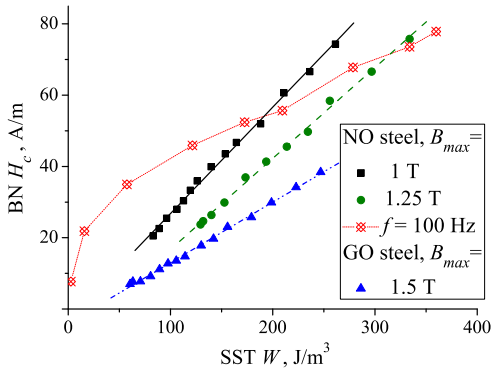

Fig. 6 Similar dependence of the BN H_c on the SST hysteresis losses, W, for the typical NO and GO steels measured at different B_{max} and f values. The fixed values of B_{max} and f are shown in the graph labels together with the parameters of the linear fits. For the sake of simplicity, the measurement with different B_{max} values was presented only for the typical NO steel and the fixed $f = 100$ Hz. The relationships for the GO steel and other f values showed the similar behavior. For the presented linear fits, the mean $R = 0.9987$ and $SD = 0.542$.

the typical steels measured with varied values of B_{max} and f. Increase of the magnetization frequency leads to deflection of the linear correlations to the BN parameter axes at $f \simeq 50$ Hz, which should be caused by a non-homogeneous strip magnetization at the higher frequencies (the BN coil detects the signal from the sample depth of about 0.1 mm) [13]. Similar deflection with B_{max} increase is probably due to a magnetic saturation: at $B_{max} \simeq 1$ T the elliptical hysteresis loops of the NO steels transform to the rectangular shaped loops (see Fig. 8).

The measurements of the different steels did not reveal any correlation of the classical BN parameters describing the level of the BN signal to the hysteresis data. The physical trend of the BN increase with increase of the magnetic hardness was evident only for the measurements of the individual steel strips with varied values of B_{max} and f [4,5]. Fig. 9 presents a typical relationship of the classical BN rms value with the SST losses.

4 Discussion

The introduced parameter, BN coercivity, demonstrates unique properties: high stability to deviations of the measurement conditions and almost perfect linear correlation to the hysteresis coercive force [3,8,12]. The parameter stability is mainly determined by its independence from the non-normalized level of the BN signal (see Figs. 2 and 3). The strong correlation of the BN H_c to the hysteresis coercive field confirms the similar nature of these magnetic effects and clarifies the physical meaning of the BN H_c as a local *surface* coercivity (see Fig. 4). It is also worth noting that another widely used BN parameter,

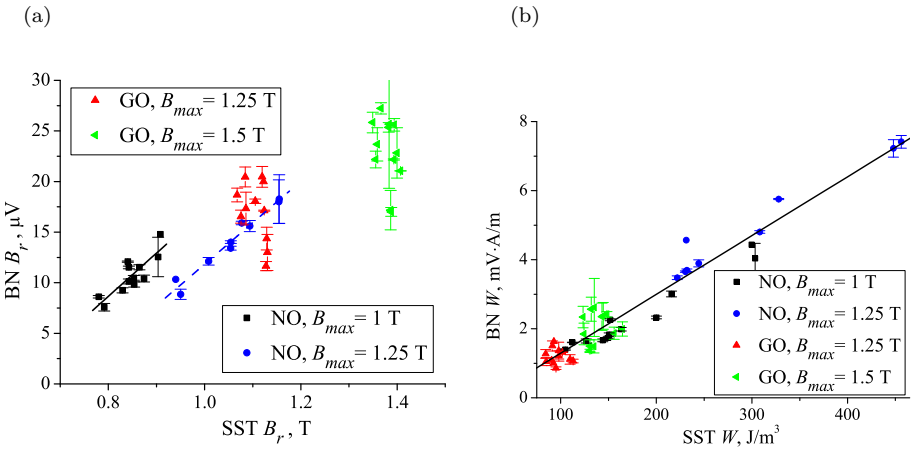

Fig. 7 (a) Relationships of the BN B_r with the SST remanent induction, B_r. The extrapolation field data are shown for all the steels, both B_{max} values and the fixed $f = 50$ Hz. The correlation coefficients of the shown linear fits: $R = 0.845$ and 0.982; $SD = 1.081$ and 0.66 for $B_{max} = 1$ and 1.25 T, respectively. (b) Similar relationship of the BN W with the SST hysteresis losses, W. The corresponding correlation coefficients are $R = 0.9691$ and $SD = 0.392$.

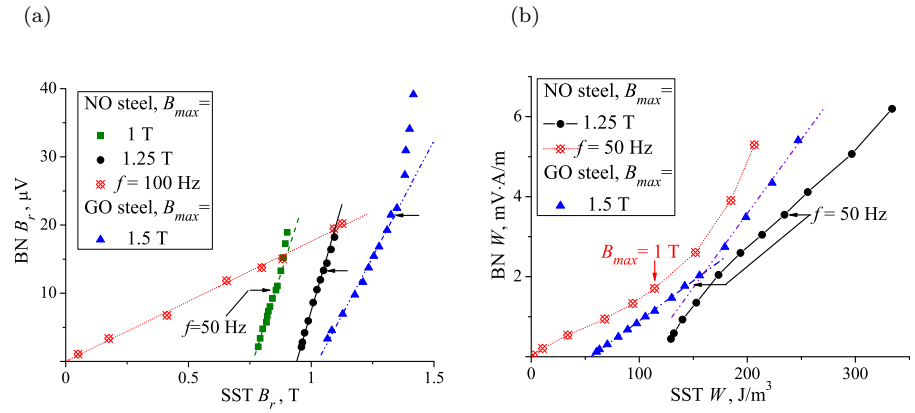

Fig. 8 Similar relationships of the BN B_r with the SST remanent induction, B_r, (a) and of the BN W with the SST hysteresis losses, W (b). The extrapolation field data are shown for the typical NO and GO steels measured at different B_{max} and f values. The fixed values of B_{max} and f are shown in the graph labels. The correlation coefficients of the shown linear fits are $R \simeq 0.998$ and $SD = 0.3 - 0.6$. The measurements with different B_{max} values were presented only for the typical NO steel and the fixed $f = 50/100$ Hz. The horizontal arrows show the data points of the measurements with $f = 50$ Hz; the vertical arrow shows the data point of the measurement with $B_{max} = 1$ T.

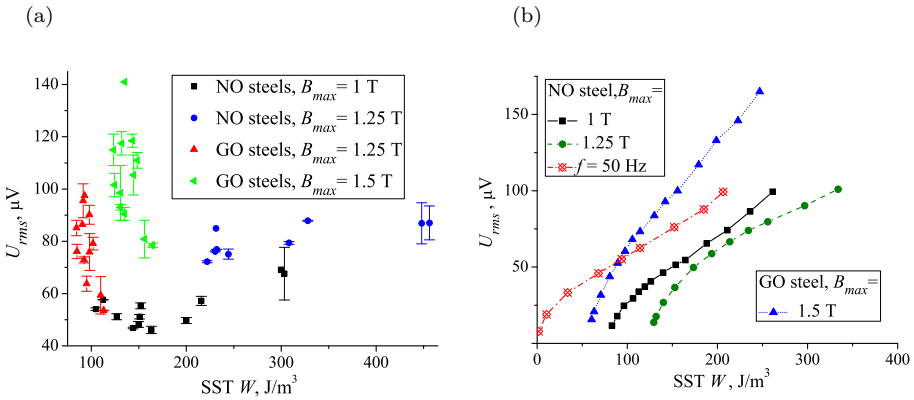

Fig. 9 Relationship of the BN rms value, U_{rms}, with the SST hysteresis losses, W: (a) for all the steels, both B_{max} values and the fixed $f = 50$ Hz; (b) for the typical NO and GO steels measured at different B_{max} and f values. The measurement with different B_{max} values was presented only for the typical NO steel and the fixed $f = 50$ Hz.

the field position of the BN envelope peak, usually shows similar behavior [9]. Discrepancy between the bulk hysteresis H_c and the surface BN H_c values can be caused by a sample sub-surface layer of different magnetic properties (surface hardening/softening) or eddy currents, as in the considered case of ac magnetization of the bulky ferromagnetic samples (see Figs. 3(b) and 8) [13].

For the NO steels, the linear correlation between the hysteresis and the BN coercivity values for the direct field data is perfectly within the reasonable level of the measurement error of a few A/m. A small offset of the correlation of $1-2$ A/m is probably caused by the above-mentioned eddy currents. However, the standard magnetization current cannot provide a reliable basis for the evaluation of the sample field in the case of the single-yoke open configuration (see Fig. 4(a)) [2,3,9]. The slightly worse relationship of the BN H_c with the SST H_c is determined by imperfections of a similar linear correlation between the direct field and the SST hysteresis measurements. These imperfections can be caused by an intrinsic error of the standard SST technique, i.e., the defined constant magnetic path l_m used for the H_i calculation. Moreover, our SST measurements were conducted through the strip insulation coating, which led to the significant decrease of the linear correlation slope for the softer GO steels. Additional measurement errors can stem from the technically complex method of the direct field measurements: calibrations of the Hall sensors, their accurate positioning, mistakes of the extrapolation procedure, etc [11,10].

The correlation between the BN H_c and the most important hysteresis parameter, W, is determined by the similar correlation between the hysteresis H_c and W. As a rule, there is a good linear correlation between the coercive force, H_c, and the losses, W, for the rectangular-shaped hysteresis loops of the electrical steels. However, the loop shape is dependent on the induction amplitude B_{max}, which leads to the similar dependence of the $H_c - W$ correlations on the B_{max} (see Figs. 5(b) and 6) [11].

The stability of other BN parameters suffers from the high decaying of the weak BN signal with small uncontrollable lift-offs of the sensing coil (see Fig. 3(a)). The weak linear correlations of the BN B_r to the hysteresis remanent induction for the NO steels confirm this fact experimentally (see Fig. 7(a)). The linearity of the correlation between the BN W and the hysteresis losses is a slightly better due to the accurate field measurement. Moreover, as opposed to the remanence relations, this loss correlation is less independent of the induction amplitude B_{max} (compare Figs. 5(b) and 7(b)). These experimental findings place special emphasis on the similarity of the hysteresis and the BN loops/signals [3]. However, because of the much higher instability of the BN B_r and W parameters compared with the BN H_c, their practical importance is rather low.

The magnetically soft electrical steels is a difficult object for the BN measurements. Structural variations between the studied electrical steels have a different influence on the BN signal level, which is illustrated by Fig. 9(a). However, for the individual steel strips with the same micro-structure, the level of the BN signal expectedly rises with the hysteresis loss increase (see Fig. 9(b)) [5]. Moreover, the BN signal is weak: the main remagnetization process in the coercivity region (fast motion of the 180° magnetic domains) occurs smoothly without significant BN activity. The typical second peak of the BN envelope is mostly responsible for the observed difference between the hysteresis and the BN loops at the saturation regions. This high-field BN activity is probably caused by an irreversible final reorganization of the magnetic domains: the formation/annihilation of the 180° and the 90° magnetic domains on the grain boundaries and in the misoriented grains (see Fig. 2) [3,14]. However, it can be also influenced by the magnetization rate: a time derivative of the measured magnetic field, dH_{ext}/dt, has a local minimum in the region of the notch, which divides the envelope peaks [8].

For the GO steels, the linear correlations between the BN and the hysteresis parameters are of much worse accuracy than that for the NO steels. However, the GO data are believed to show the same trend, which is demonstrated by the qualitatively similar correlations between the BN H_c and the SST H_c or W as well as by the good positioning of the GO data on the BN-SST loss relationship (see Figs. 5 and 7(b)). The lower correlation accuracy for the magnetically softer GO steels is caused by a higher relative measurement error and a lower range of the magnetic parameter variation for the different steel grades. This suggestion is proved by the good linear correlations for the measurements of the typical GO steels in much wider range of the parameter variation (see Figs. 4(b), 6 and 8). Another principal problem is a higher magnetization inhomogeneity of the larger grains of the GO steels, which can lead to a higher scattering of the field data measured by the Hall sensors with the much smaller sensitive area [3,10].

Therefore, in this stage of the setup development, the BN technique can be used only for rough evaluation of the magnetic properties of GO steels. Moreover, the accurate measurement of NO steels with the 3000 cycle averaging takes one minute, which is not appropriate for on-line testing. More

accurate and fast measurements require a different low-noise field sensor with a larger sensitive area. This should improve the accuracy of the GO steel measurements to an acceptable level. For further development of the presented laboratory setup to an on-line testing system, the Hall sensors used should be replaced by a classical H-coil or by modern magneto-resistive/flux-gate sensors, which have already demonstrated better performance [10,15]. However, the Hall sensors can also be used in practice for the dc magnetic testing of harder construction steels [8,13].

5 Conclusion

Simultaneous *local* measurements of the surface sample field and the Barkhausen noise signal make it possible to stabilize the recently introduced magnetic parameter, called Barkhausen noise coercivity. This parameter shows high stability with respect to variations of the experimental conditions: the sensing coil lift-off, its design, the yoke-sample gap and the magnetization frequency. This parameter also demonstrates the strong linear correlations to the hysteresis coercive force and to the hysteresis losses of the electrical steels measured by the standard single sheet tester at 50 Hz sinusoidal magnetization. This is valid only with reference to the directly measured field; the common current field method cannot be used for the magnetically open circuits. This finding provides a new opportunity for the non-contact local evaluation of the ac magnetic hysteresis properties of electrical steels directly on the production line.

Acknowledgements The author appreciates the financial support of the Czech Science Foundation (GACR) under projects 102/09/P108 and 13-18993S.

References

1. Matyuk VF, Goncharenko SA, Hartmann H, Reichelt H (2003) Modern state of non-destructive testing of mechanical properties and stamping ability of steel sheets in a manufacturing technological flow. Russ J Nondestr Test 39:347–380.
2. Iranmanesh H, Tahouri B, Moses AJ, Beckley P (1992) A computerised Rogowski-Chattock potentiometer compensated on-line power-loss measuring system for use on grain-oriented electrical steel production lines. J Magn Magn Mater 112:99–102.
3. Stupakov O, Perevertov O, Stoyka V, Wood R (2010) Correlation between hysteresis and Barkhausen noise parameters of electrical steels. IEEE Trans Magn 46:517–520.
4. Birsan M, Szpunar JA, Krause TW, Atherton DL (1996) Correlation between the Barkhausen noise power and the total power losses in 3% Si-Fe. J Appl Phys 79:6042–6044.
5. Patel HV, Zurek S, Meydan T, Jiles DC, Li L (2006) A new adaptive automated feedback system for Barkhausen signal measurement. Sens Actuator A-Phys 129:112–117.
6. Xin Q, Shu D, Wei W, Chen J (2012) Magnetic Barkhausen noise, Metal Magnetic Memory testing and estimation of the ship plate welded structure stress. J Nondestruct Eval 31:80–89.
7. Franco FA, González MFR, Campos MF, Padovese LR (2013) Relation between magnetic Barkhausen noise and hardness for Jominy quench tests in SAE 4140 and 6150 steels. J Nondestruct Eval 32:93–103.

8. Stupakov O, Pal'a J, Takagi T, Uchimoto T (2009) Governing conditions of repeatable Barkhausen noise response. J Magn Magn Mater 321:2956-2962.
9. Boller C, Altpeter I, Dobmann G, Rabung M, Schreiber J, Szielasko K, Tschuncky R (2011) Electromagnetism as a means for understanding materials mechanics phenomena in magnetic materials. Mat-wiss u Werkstofftech 42:269–278.
10. Stupakov O (2012) System for controllable magnetic measurement with direct field determination. J Magn Magn Mater 324:631–636.
11. Stupakov O (2012) Controllable magnetic hysteresis measurement of electrical steels in a single-yoke open configuration. IEEE Trans Magn 48:4718–4726.
12. Stupakov O (2013) Barkhausen noise sensor with direct field control. Sens Lett 11:209–212.
13. Stupakov O, Perevertov O, Tomáš I, Skrbek B (2011) Evaluation of surface decarburization depth by magnetic Barkhausen noise technique. J Magn Magn Mater 323:1692–1697.
14. Perevertov O, Schäfer R (2012) Influence of applied compressive stress on the hysteresis curves and magnetic domain structure of grain-oriented transverse Fe-3%Si steel. J Phys D: Appl Phys 45:135001 (11pp).
15. Cheng W (2012) Pulsed eddy current testing of carbon steel pipes wall-thinning through insulation and cladding. J Nondestruct Eval 31:215–224.